Efficient Conversion of the Energy of Intense Relativistic Electron Beams into rf Waves

M. Friedman, R. Fernsler, S. Slinker, R. Hubbard, and M. Lampe
Plasma Physics Division, Naval Research Laboratory, Washington, D.C. 20375
(Received 5 April 1995)

A novel relativistic klystron amplifier has achieved 50% energy efficiency, a significant advance over the previous state of the art of 20%. A radially converging structure that was inserted in the output gap reduced the potential energy residing in the electron beam and maximized rf output energy. Electrons that stopped inside the gap were intercepted by this structure and were shunted to ground. This is in contrast to classical klytons in which such electrons would have formed a virtual cathode and/or flow backward, regaining energy from the rf field.

PACS numbers: 85.10.Jz, 41.75.Ht

A high current "conventional" klystron amplifier has been considered as a candidate for a high power microwave (HPM) source [1]. However, klystrons that operate with high current are inefficient due to space charge effects and the large spread in the electron energy at the output gap. To reduce these effects a high beam voltage is required. But high voltage leads to beam stiffness that can be overcome only by injecting a high rf input power and/or by lengthening the drift region in klystrons.

Relativistic klystron amplifiers (RKA's) use the self-field of annular intense relativistic electron beams (IREB's) to considerably reduce effects associated with beam stiffness [2,3], but the efficiency is still limited by beam loading, rf breakdown, and the spread in the electron kinetic energies at the gaps.

During the last year, we have developed a new type of RKA [4] that employs cavities with inductively loaded wide gaps. Using these cavities, we eliminated many deleterious effects that plagued the operation of narrow gap RKA's in the past. However, the energy distribution of the electrons at the output gap could not be narrowed down, leading to inefficient operation. The spread in kinetic energy results from the spatial distribution of the potential energy residing in the IREB and from the bunching mechanism. The particle code MASK [5], which successfully simulated the global operation of RKA's [4], was used to obtain microscopic details of the modulated IREB such as density and energy distributions of the electrons [Fig. 1(a)–1(d)].

To achieve efficient operation of RKA (or any klystron-like devices), the rf voltage across the output gap has to fulfill two conditions that are impossible to satisfy at the same time, especially for a modulated beam with a large energy spread: (1) It has to be low enough to avoid electron reflection that can cause a virtual cathode formation. (2) It has to be high to drain most of the electrons' energy so as to maximize the RF energy output. An energy efficienty of 20% and a power efficiency of 35% were obtained for RKA's at the Naval Research Laboratory [6]; similar efficiencies were obtained at Los Alamos National Laboratory [7] and at Physics International [8].

In this Letter we will describe a mechanism that substantially increases the energy efficiency of RKA's to 50%.

The experimental apparatus is shown in Fig. 2. Three gaps, each 10 cm long, were inserted in a smooth wall drift tube of radius $r_w = 6.7$ cm. An electron beam propagating through an empty gap of such a length would have acquired a large potential energy. A reduction of the potential energy was achieved [4] by inserting structures inside the empty gaps. These structures consisted of a stack of 23 metallic washers of thickness 0.075 cm and of outer radius $r_{w2} = 9.2$ cm. The inner radius of the washers inserted in the first two gaps was $r_{w1} = 6.7$ cm ($= r_w$). The inner radii of the washers in the

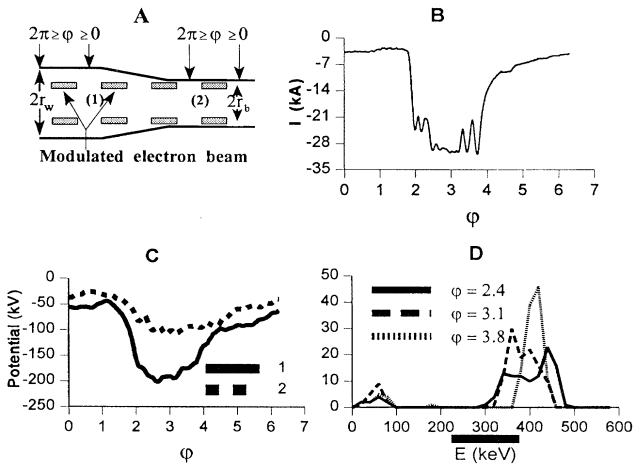

FIG. 1. (A) A section of the simulation geometry displaying a modulated electron beam propagating in an axisymmetric drift tube. The position of an electron within a bunch is defined by a phase angle φ. At the center of a bunch, $\varphi = \pi$, and at the middle between two bunches, $\varphi = 2\pi$ or 0. (B) A current profile of a single bunch located at an axial position where the rf current amplitude reached its maximum. (C) Potential energy residing in the bunch displayed in (B) calculated for the innermost electrons and at an axial position where $r_w = 6.7$ cm (position 1) and $r_w = 6.4$ cm (position 2). (D) Electron kinetic energy distribution of the bunch displayed in (B): at $\varphi = 2.4$, $\varphi = 3.1$, and $\varphi = 3.8$.

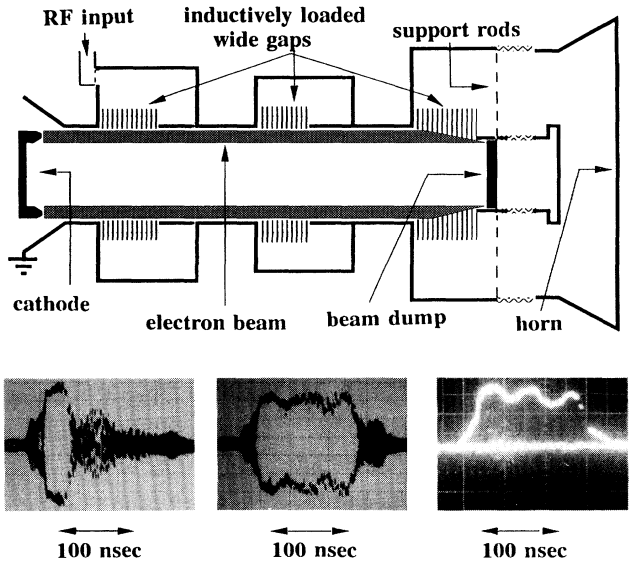

FIG. 2. (Top) Schematics of the experiment. (Bottom left) The rf output electric field signal for $B_z = 8$ kG. (Bottom middle) The output rf electric field signal, $B_z = 3$ kG. (Bottom right) rf output power sampled by a crystal detector, $B_z = 3$ kG.

third gap changed sequentially from 6.7 to 6.2 cm. The IREB was stopped after crossing the third gap and the next-to-the-last washer. The washers were supported by four thin metallic rods mounted at radius $r_{\text{rod}} = 8.9$ cm connected across each gap. The first two gaps were connected to coaxial cavities tuned to 1281 MHz. The third gap was connected to a "leaky" cavity consisting of a coaxial transmission line with one end of the inner electrode serving as the electron dump. The inner electrode was supported downstream, at a null point of the standing wave, by six radial rods. The other end of the inner electrode was connected to a metallic disk. The resonant frequency ω, the quality factor Q, and the shunt impedance $\Re$ of this cavity were tuned by changing the position and radius of the disk. The outer electrode was connected to a radiating cylindrical horn with a 1 m diameter window. This third cavity is the rf converter. The apparatus was immersed in a quasi-dc magnetic field, B_z, and was evacuated to base pressure $<10^{-5}$ Torr. A diode injected an annular IREB of radius $r_b = 6.1$ cm, thickness 0.3 cm, and current $I_0 = 11$ kA into the system. The maximum voltage pulse applied to the diode was 450 kV. The pulse duration was 130 ns at maximum voltage, with a voltage rise time of 30 ns and a fall time of 50 ns.

The rf waves at the resonant frequency penetrated easily into (and out of) the cavities through the inductive structures, establishing a bidirectional electric field mode inside the wide gaps. This mode ensured a synchronized interaction between the rf and the electrons [4]. A high level of current modulation downstream of the first gap was observed when a rf pulse of power, $P_{\text{in}} = 4$ MW, was externally injected into the first cavity. The second gap was inserted at the axial position where the rf current reached a maximum. The beam was fully modulated downstream of the second gap. Radiated power was maximized by choosing the site of the third gap at an axial position where the first harmonic of the beam modulated current reached its peak ($\sim$14 kA), and by adjusting the geometry of the converter. The output rf pulse emitted from the conical antenna was sampled by a small horn. The electric field established in the receiving horn was displayed on a Tektronix oscilloscope model SCD 5000.

The principal result of the experiment was that the peak output power was $P_{\text{out}} = 2.85 \pm 0.15$ GW, or about 60% *power* efficiency independent of the magnetic field intensity. When an 8 kG magnetic field intensity was used, the output rf pulse duration was shorter (50 ns) than the input electrical pulse (Fig. 2, bottom left). At lower magnetic field intensities the output pulse duration lengthened, and it reached the full input electrical pulse duration at $B_z \approx 3$ kG (Fig. 2; bottom, middle and right). At this level of magnetic field intensity the *energy* efficiency of the device was 50%. Changing the frequency of the external input rf by ± 5 MHz reduced the output power by 3 dB.

The high efficiency and the low solenoidal field needed to focus the IREB have never before been observed in narrow-gap RKA's. These experimental results are explained below.

It had previously been shown [9] that, at a critical magnetic field intensity, the propagation of a magnetically focused annular IREB inside a smooth drift tube could be disrupted by inserting a single small wall perturbation. The energy of any electron inside the drift region $(\gamma_{\text{inj}} - 1)m_0c^2$ is shared between kinetic energy $(\gamma_0 - 1)m_0c^2$ and potential energy $\Phi = (m_0c^2)I_0/I_s\beta_\parallel$, where I_0 is the beam current, $I_s = (2\pi\epsilon_0 m_0 c^3)/e \ln(r_w/r_b)$, $\beta_\parallel = v_\parallel/c$, and $v_\parallel$ is the beam velocity parallel to the magnetic field. The kinetic energy can be divided into parallel kinetic energy $E_\parallel$ and perpendicular kinetic energy $E_\perp$. At the vicinity of a wall perturbation, the potential energy residing in the IREB increases, thus slowing down the electrons and reducing their kinetic energy. While propagating through the potential hill, electrons gain rotational velocity under the combined influence of an increased radial (self-) electric field and the axial (external) magnetic field. The gain in perpendicular energy is balanced by a drain from the parallel energy. Since the rotational energy increases with a decrease in B_z, at a critical magnetic field the drain on the parallel energy is so large that electrons stop, and a virtual cathode is formed.

In narrow gap RKA's, wall perturbations (i.e., gaps) were inserted in the drift tube walls. A strong axial mag-

netic field (10 kG) was needed for RKA's to perform stably. At low magnetic field intensity a virtual cathode was formed, and the RKA mechanism was disrupted. When the narrow gaps were replaced by the inductively loaded wide gaps, the potential hill was almost eliminated. Here, a lower magnetic field intensity (3 kG) was sufficient for the RKA to operate.

The large improvement in the energy efficiency of the wide gap RKA at a 3 kG magnetic field can be explained by examining the radial motion of test electrons. These electrons are located on the beam envelope and are under the influence of the self-field and applied electric and magnetic fields. The electron's position (r, z) inside the gap can be evaluated from the radial force equation applicable for an immersed cathode and azimuthal symmetry:

$$\frac{d}{dt}\left[\gamma_p m_0 \frac{dr}{dt}\right] = \frac{\mu_0 e I c}{2\pi r}\frac{I - \beta_p\beta_b}{\beta_b} - 0.25\gamma_p m_0 \omega_{ce}^2\left[I - \left(\frac{r_0}{r}\right)^4\right]r,$$
$$z = z_0 + \int \beta_p c\, dt, \qquad (1)$$

where z_0 is the position of the gap entrance, r_0 is the initial radial position of the test electron, $\omega_{ce} = eB_z/\gamma_p m_0$, $\beta_J = v_J/c$ [the subscript J stands for $b(=$ beam) or $p(=$ test particle)], and v_b, v_p are the beam and the test electron velocity. By neglecting rotational and radial energies, one obtains $\beta_J = (1 - \gamma_J^{-2})^{1/2}$. The kinetic energy $(\gamma_J - 1)m_0c^2$ was calculated from the injected energies $(\gamma_{J,\mathrm{inj}} - 1)m_0c^2$, from the height of the potential hill, and from the axial voltage across the gap:

$$\gamma_{J,\mathrm{inj}} = \gamma_J + \frac{I}{I_s\beta_b} + \frac{e}{m_0c^2}\int \mathcal{E}_z\, dz. \qquad (2)$$

The instantaneous beam current can be expressed as $I = I_0(1 + \Sigma[A_n \sin(n\omega t) + B_n \cos(n\omega t)])$, where A_n and B_n are time independent coefficients. The electric field along the gap $\mathcal{E}_z$ consisted of two components: (1) an inductive electric field that originated from the transitlike interaction of a bunch with the inductive structure [4], and (2) a resistive bipolar field $\mathcal{E}_R \cos(\pi z/D)$, where $\mathcal{E}_R = \Re I_0 A_1 \sin(\omega t + \varphi)$, $\Re$ is the shunt impedance, D is the gap length, $z = v_p t$, and φ is the phase [see Fig. 1(a)] of the test electron. When $\beta_b = \beta_p$ Eq. (1) is the envelope equation for a modulated IREB propagating through a wide gap. Equation (1) was solved numerically for test electrons with initial energies greater, smaller, and equal to the beam electron energy. The following results are general in nature.

(1) The radial position r of the test electrons was an oscillatory function of the axial distance z (Fig. 3). The amplitude and wavelength of the oscillations grew with $1/B_z$ and with the instantaneous beam current I. The largest amplitude occurred at the third gap, where the peak modulated current is maximum.

(2) There were three classes of test electrons: (a) electrons that crossed the whole length of the gap, losing or gaining energy depending on the injection phase, (b) electrons that moved axially forward but intersected the radially converging structure located in the gap (A in Fig. 3 left), and (c) electrons that lost all their *kinetic* energy before reaching the end of the gap and reflected backward ($\beta_b > 0$, $\beta_p \leq 0$). These electrons were affected by a *repulsive* electric force and a *repulsive* magnetic force generated by the IREB. The combined force displaced the test electrons radially. The lower the applied axial magnetic field, the larger the displacement. At 3 kG the test electrons with $\beta_p \leq 0$ moved in an almost purely outward radial motion before being intercepted by the radially converging structure (Fig. 3, right). At a high magnetic field (e.g., 8 kG) these electrons moved almost collinearly, missing the walls or structure and gaining energy from the RF field (B in Fig. 3, left).

(3) The radially converging axisymmetric grounded structure used in the converter transformed the beam potential energy to electron kinetic energy as the beam propagated along the wide gap. The simulation code confirmed the reduction in the potential energy residing in the IREB and the increase in electron kinetic energy as the modulated beam propagated in the radially converging drift region [Fig. 1(c)]. Note that only kinetic energy can be converted into rf.

(4) By optimizing the experimental parameters (e.g., electric and magnetic field intensities), test electrons with $\gamma_{p,\mathrm{inj}}$ that satisfy $\gamma_{b,\mathrm{inj}} + 0.4 > \gamma_{p,\mathrm{inj}} - 0.4$ lost >60% of their energy to the rf field and were stopped by the walls or structure without reflection. At higher B_z most of the test electrons still lost >60% of their enregy, but some of them were reflected. Their number increased with B_z. These reflected electrons were the "seed" needed for a virtual cathode formation. The time τ taken to form a virtual cathode shortened as the number of reflected electrons increased (i.e., as B_z increased). The rate of energy lost $(= P)$ by the beam to the rf field did not depend on B_z for a time $<\tau$. At the onset of a virtual cathode, $P = 0$. Hence the total of rf energy $P\tau$, maximized at a low value of B_z (when τ is greater than the beam duration), was observed experimentally.

Note that one gets from Eq. (1) the trajectory of an individual test electron but not the behavior of the whole beam if a large part of it reflects.

To estimate the system efficiency we assumed that the beam and the test electrons have the same energy (500 keV). The current profile was taken from Fig. 1(B). We approximated the modulated current as a train of $\cos^2$ pulses. Each pulse had a base-to-base width of 0.45 of the period and a peak current of around $I = 29$ kA. A dc current of 1 kA was superimposed on the modulated current. The efficiency was set equal to the sum of all the energies lost by test electrons (which were injected with phases between 0 and 2π), divided by the sum of their initial energies. The efficiency was optimized by varying

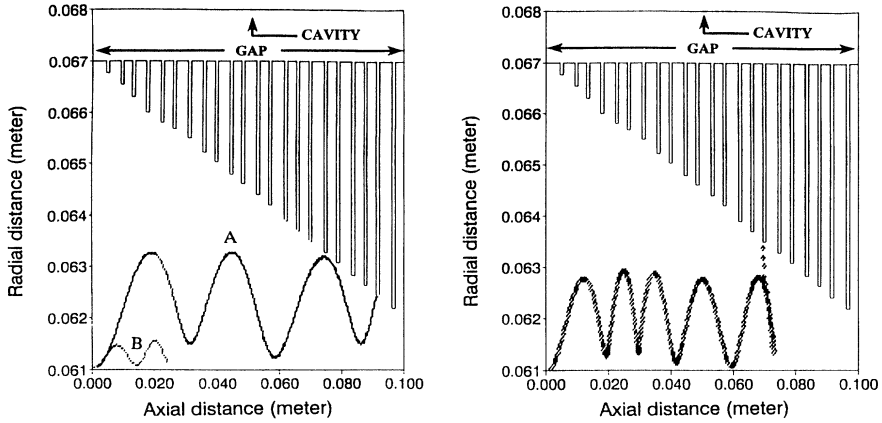

FIG. 3. (Left) Trajectories of 500 keV test electrons, $\varphi = \pi$, traversing the output gap. (A) $B_z = 3.6$ kG and (B) $B_z = 8$ kG. (Right) Trajectory of a 375 keV test electron transversing the output gap, $\varphi = 0.8\pi$, $B_z = 3.6$ kG. At $B_z = 3.6$ kG the test electrons lost >65% of their total energy crossing the gap.

the amplitude of the gap axial electric fields. Cases were rejected when any test electron was reflected and not absorbed by the structure. Under these conditions we obtained a maximum of ≈65% efficiency with a magnetic field intensity of 3.6 kG.

In conclusion, we have shown that wide gap RKA's can be efficient sources for rf. We believe that the same mechanisms can also be employed in high power classical (nonrelativistic) klystrons, provided an annular beam is used. With such a system, klystron efficiency can be increased without resorting to depressed collector techniques.

This work was supported by ONR.

[1] For example, see P. B. Wilson, in *Physics of High Energy Particle Accelerators,* edited by R. A. Carrigan, F. R. Huson, and M. Month, AIP Conf. Proc. No. 87 (AIP, New York, 1982, pp. 450–563.

[2] M. Friedman and V. Serlin, Phys. Rev. Lett. **55**, 2860 (1985).

[3] V. Serlin *et al.,* IEEE Trans. Plasma Sci. **22**, 692 (1994), and references within.

[4] M. Friedman *et al.,* Phys. Rev. Lett. **74**, 322 (1995).

[5] A. Palevsky and A. Drobot, in *Proceedings of the Ninth Conference on the Numerical Simulation of Plasmas,* Northwestern University, Evanston, IL, 1980 (unpublished).

[6] M. Friedman *et al.,* Rev. Sci. Instrum. **61**, 171 (1990).

[7] M. V. Fazio *et al.,* IEEE Trans. Plasma Sci. **22**, 740 (1994).

[8] J. S. Levine and B. D. Harteneck, Appl. Phys. Lett. **65**, 2133 (1994).

[9] M. Friedman, Appl. Phys. Lett. **24**, 303 (1974).

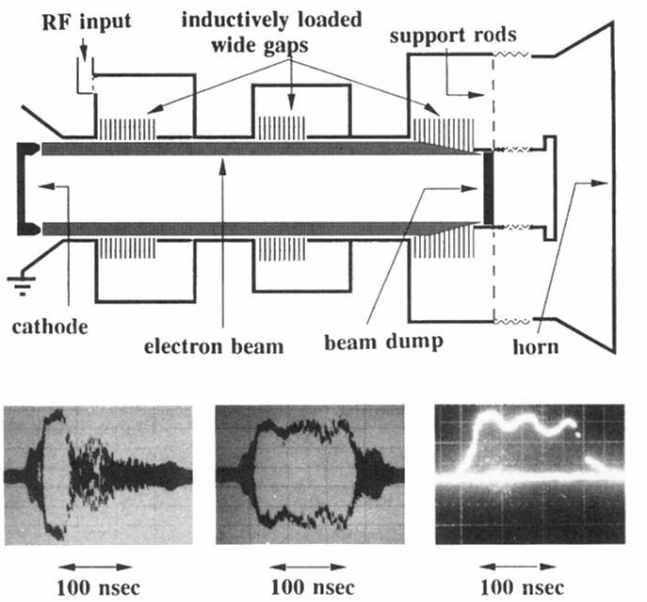

FIG. 2. (Top) Schematics of the experiment. (Bottom left) The rf output electric field signal for $B_z = 8$ kG. (Bottom middle) The output rf electric field signal, $B_z = 3$ kG. (Bottom right) rf output power sampled by a crystal detector, $B_z = 3$ kG.